OPEN ACCESS
JOURNAL OF ADVANCED DIELECTRICS
Vol. 11, No. 1 (2021) 2150002 (7 pages)

DOI: 10.1142/S2010135X21500028

Synthesis and characterization of strontium-doped barium titanate thin film by dip and dry technique

S. G. Chavan*, A. N. Tarale† and D. J. Salunkhe*,‡

*Nano-composite Laboratory, Department of Physics
Karmaveer Bhaurao Patil Mahavidyalaya
Pandharpur, Solapur, India

†Science College Pauni Dist. Bhandara-441910, India

‡salunkhedj@rediffmail.com

Received 19 April 2020; Revised 13 December 2020; Accepted 14 December 2020; Published 19 January 2021

Thin films of polycrystalline $(Ba_{1-x}Sr_x)TiO_3$ ($x = 0.2$ and 0.3) with Perovskite structure were prepared by a dip and dry technique on a platinum-coated silicon substrate. The good quality thin films with uniform microstructure and thickness were successfully produced by dip-coating techniques annealed at 730 °C for 1 h. The resulting thin film shows a well-developed dense polycrystalline structure with more uniform grain size distribution. The BST thin films were characterized for their structural, Raman spectroscopy, morphological properties, and complex impedance properties. The dielectric constant-frequency curve showed the good dielectric constant and loss dielectric loss with low-frequency dispersion. The BST 0.3 thin film reveals that the dielectric constant and dielectric loss at a frequency of 1 kHz were 578 and 0.02, respectively. The obtained results on dielectric properties can be analyzed in terms of the Maxwell–Wagner model.

Keywords: Ceramics; sol–gel synthesis; thin film; dielectric properties.

1. Introduction

$(BaSr)TiO_3$ is a well-known perovskite material due to its excellent dielectric and ferroelectric properties.[1–4] As the doping level of Sr increases in the $BaTiO_3$ (BT), the Curie temperature (Tc) decreases. $Ba_{1-x}Sr_xTiO_3$ (BST) is a technologically important ferroelectric material due to its many applications such as tunable filter, microwave phase shifters, oscillators, and varactors.[1–7] The main application of the research on BST thin film has storage capacitors in dynamic random-access memory (DRAM).[2,7] The BST is an important dielectric material that shows high dielectric constant, low leakage current, low dielectric loss, and the composition-dependent transition temperature.[7,8] The variety of deposition methods have been tried out for deposition of BST thin film including sol–gel, laser ablation, chemical vapor deposition (CVD), and r.f.-sputtering.[7,11–13] The BST ferroelectric thin films prepared by the polymeric precursor method have a number of advantages over other methods such as (1) good compositional homogeneity, (2) low cost, (3) high purity, and (4) relatively low processing temperatures and the ability to coat large substrate areas.[7,9,14,15]

In this work, we report the synthesis and characterization of BST thin film on platinum substrate by using dip and dry deposition technique to achieve homogeneous, crack-free, nano-sized, smooth $Ba_{0.8}Sr_{0.2}TiO_3$ and $Ba_{0.7}Sr_{0.3}TiO_3$ thin films at 730 °C for 1 h. The Pt (111)/Ti bilayer has been widely used as a bottom electrode for the ferroelectric thin film deposition. The TiO_2 buffer layer is introduced to promote adhesion between Pt and Si substrate.[9,10] Other advantages of using the Pt-coated substrate are that Pt electrode has good stability in high-temperature oxidizing environments, high electrical conductivity, and low leakage current.

2. Experimental

The BST0.2 and BST0.3 thin films are synthesized using the acetate-alkoxide route. Barium acetate ($Ba(CH_3COO)_2$) (S d fine, AR grade 99%), Strontium acetate ($Sr(CH_3COO)_2$) (Aldrich 99%), Titanium isopropoxide ($Ti[OCH(CH_3)_2]_4$) (Aldrich 97%), 2-methaoxyethanol (Thomas Baker, AR grade 99.5 %) and acetic acid (CH_3COOH) (Loba Chemie, AR grade 99.7%) were used as starting material. The stoichiometric amount of barium acetate in the 10 ml acetic acid solution and strontium acetate in the 10 ml acetic acid solution were added into the solution (Ba/Sr ratio was fixed at 70/30 and 80/20). A stoichiometric amount of titanium iso-propoxide was mixed uniformly in 2-methaoxyethanol. The acetate and alkoxide solution were mixed together. The mixture thus obtained was heated at 40 °C for 4 h. The total volume up to 60 ml is adjusted by adding 2-methaoxyethanol to achieve an

‡Corresponding author.

appropriate viscosity for the purpose of dip coating. The Pt/TiO_2/SiO_2/ *n*-si (100) substrates are used for the purpose of thin-film deposition. The thin films are grown using a dip and dry technique followed by pyrolysis at 400 °C and annealing at 730 °C for 1 h in a conventional furnace.

The BST thin films were carried out for X-ray Diffraction, Raman Spectroscopy, FESEM, and dielectric measurement. The crystal structure of BST thin film was carried out by X-ray diffractogram (Bruker D8 Advance X-ray diffractometer Pune). The electrical properties measurement was performed using a Wyne Kerr LCR-Q meter (6500 B). Renishaw Raman spectroscope is used to record Raman spectra. The RL532C LASER source is used to record Raman spectra.

3. X-Ray Diffraction of BSTx Thin Film

Figures 1(a) and 1(b) show X-ray diffractogram of thin films of BST0.2 and BST0.3, respectively. The films are deposited on pt/TiO_2/SiO_2/*n*-si (100) substrates using a dip and dry technique. From Figs. 1(a) and 1(b), it could be seen that the films grown are phase pure and polycrystalline in nature. All the XRD peaks match well with standard JCPD data card number 34-0411 of the BST.4. The XRD peaks corresponding to (100), (110), (111), (200), (210), and (211) planes are indexed at respective refection angle 2θ. The peaks at 2θ equal to 33, 47, 54, 61, and 70 corresponds to Si(100). However, an intense peak at 39° corresponds to (111) plane of Platinum (pt). From XRD plots, it is seen that the intensity of (110) plane is maximum in both the cases, BST0.2 and BST0.3, which indicate that the BST films on Pt/Si (100) substrates prefer (110) direction oriented growth. However, the peaks corresponding to (200), (210), (211) planes show exhibits of a tetragonal distortion. Therefore BST0.2 and BST0.3 are observed to exhibit pseudo-cubic crystal structure with a tetragonal distortion. From Figs. 1(a) and 1(b), from the XRD data, it is seen that the BST0.2 exhibits tetragonal crystal structure, while BST0.3 possesses cubic crystal structure. The interplanar distance "*d*" is calculated using Brags law as follows:

$$d = n\lambda \mathrm{Sin}\theta,$$

where *d* is the interplanar distance, *n* is an order of reflection, θ is the angle of reflection and λ is the wavelength of X-ray source Cu($k\alpha$). Further, the calculated "*d*" value is used for the determination of lattice parameters "*a*" and "*c*" of BST thin films. The lattice parameters are calculated using the following formula:

$$1/d^2 = (h^2 + k^2 + l^2/a^2).$$

The calculated lattice parameter "*a*" for the BST0.2 is 3.9814 Å, while the lattice parameters "*a*" for the BST0.3 are 3.9761 Å.

From XRD data, crystallite size is calculated using Scherrer's formula as follows:

$$D = \frac{k\lambda}{\beta \cos\theta},$$

where *D* is the crystallite size, *k* is the constant, equal to 0.9, λ is the wavelength of the copper (Cu), β is the full width half maxima (FWHM), and θ is the angle of reflection. The calculated values of average crystallite size for BST0.2 and BST0.3 are 47 and 49 nm, respectively.

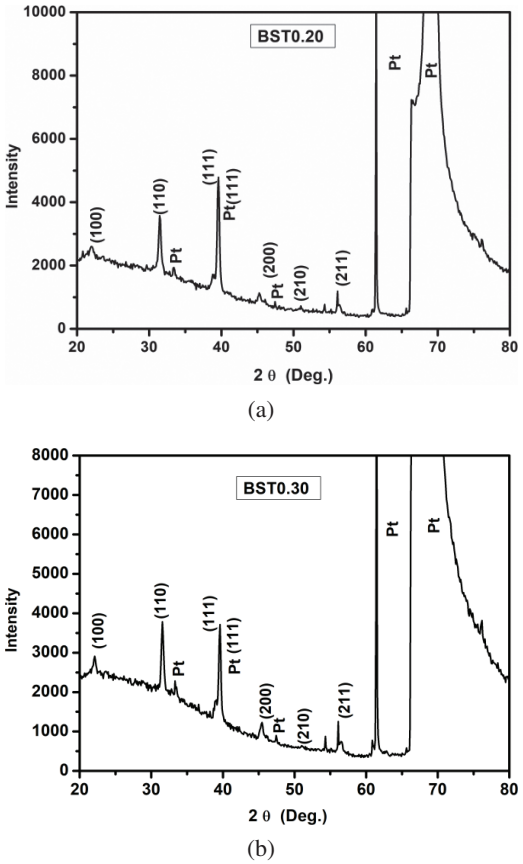

Fig. 1. (a) X-ray diffractogram of BST0.20 thin film. (b) X-ray diffractogram of BST0.30 thin film.

4. Raman Spectroscopy

Raman spectroscopy is used to investigate the transition between vibrational energy levels in the pervoskite oxide systems. This technique gives information about the chemical bonds, anharmonicity, and phase transition. Figures 2(a) and 2(b) show the room temperature Raman spectra for BST0.2 and BST0.3 thin films deposited on a Pt/TiO_2/SiO_2/*n*-si (100) substrates, respectively. The observed Raman peaks are indexed using earlier reports on BST thin films. The observed Raman peaks for BST0.2 thin films at various wavenumbers are 236, 303, 545, 610, and 745 cm^{-1}, while for BST0.3 are around 227, 293, 560, and 728 cm^{-1}. In both cases, a sharp peak is observed in the vicinity 520 cm^{-1},

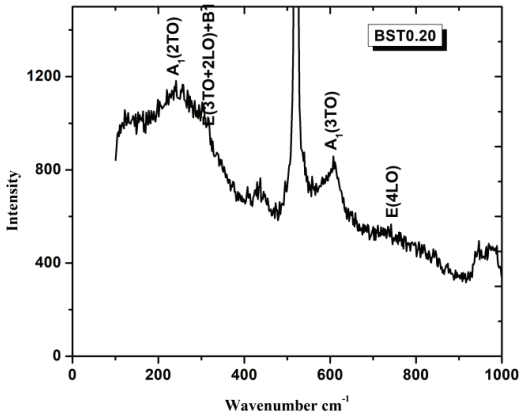

(a)

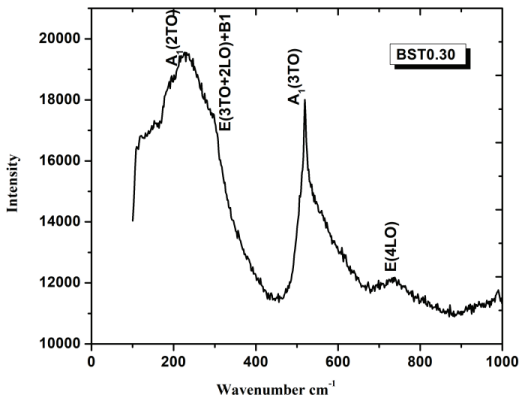

(b)

Fig. 2. Raman spectra of $Ba_{1-x}Sr_xTiO_3$ thin films (a) for $x = 0.2$ and (b) $x = 0.3$.

which is attributed to Si(100) substrate. The Raman spectra of BST0.2 and BST0.3 films were compared with spectra of $BaTiO_3$ and peaks at 303, 293, 745, and 728 cm^{-1} were seen, which confirm the tetragonal structure.[16] All the peaks were attributed to the Raman active modes of the BST0.2 and BST0.3.[16] These results have similarities to the earlier reports.[17,18]

5. FESEM Images BSTx Thin Films

Figures 3(a) and 3(b) show the FESEM images with magnification unit is 7000 and 5000 K for BST0.2 and BST0.3, respectively. The surface morphology shows the surface of BST0.3 and BST0.2 thin films are seen to be fairly uniform and particle size for BST0.2 and BST0.3 is 40 nm. The FESEM images of thin films show a rather good density of grains without cracks for this case three successive layers of each BSTx are deposited for further investigations of the electrical properties. Figure 4 shows a cross-section image of BST0.30 thin films. From this image, it is seen that the thickness of BST0.30 thin film is 630 nm for three layers.

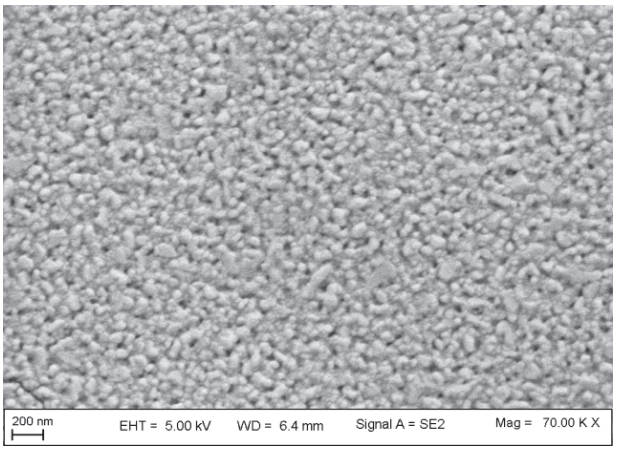

(a)

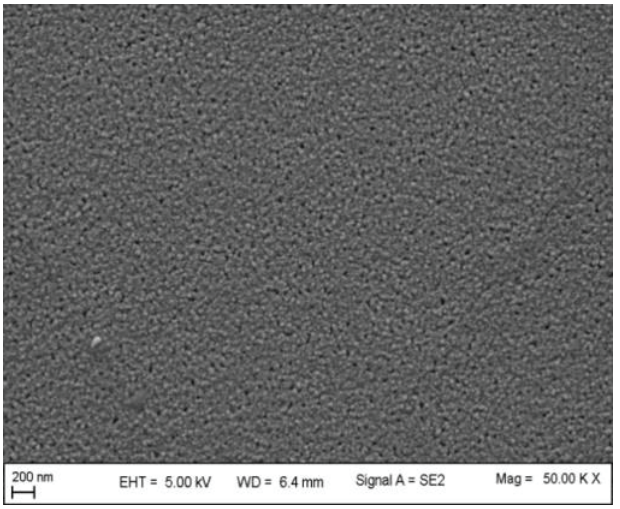

(b)

Fig. 3. (a) FESEM micrograph of BST0.2. (b) FESEM micrograph of BST0.3.

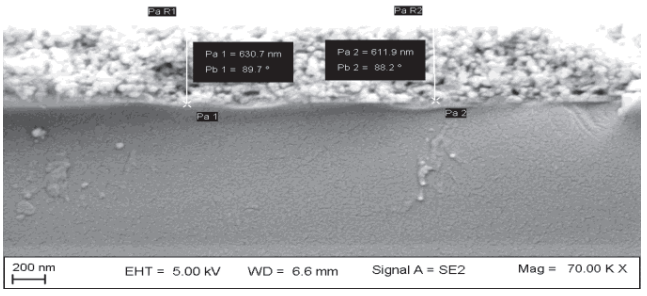

Fig. 4. Cross-sectional image of BST0.30.

6. Dielectric Properties

The dielectric properties of the BST0.2 and BST0.3 thin films are determined at room temperature as a function of frequency. Figures 5(a) and 5(b) show the variation of dielectric constant and dielectric loss as a function of frequency

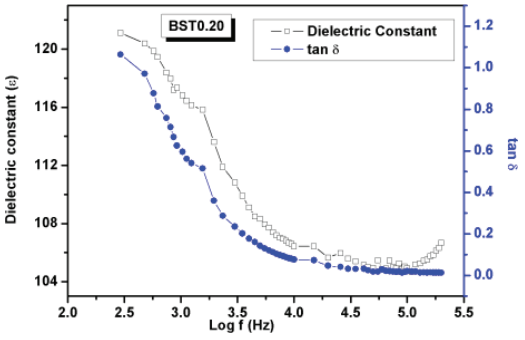

(a)

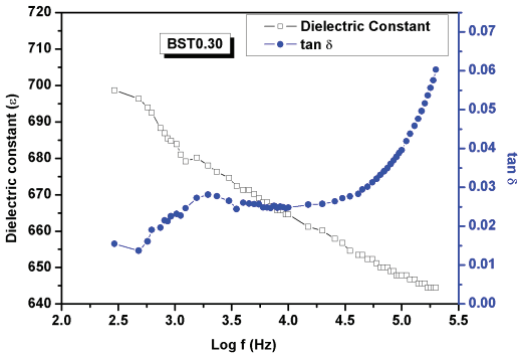

(b)

Fig. 5. (a) Variations dielectric constant (ε) and loss tangent (tan δ) with frequency for BST0.2. (b) Variations dielectric constant (ε) and loss tangent (tan δ) with frequency for BST0.3.

(log f) for the BST0.2 and BST 0.3 thin films, respectively. In Figs. 5(a) and 5(b), the y-axis on the left side of the figure represents the dielectric constant, while y-axis on the right side of the figure represents the dielectric loss (tan δ). From Fig. 5(a), it is observed that the dielectric constant ε for BST0.2 thin film decreases with increase in frequency and relaxation behavior are observed at lower frequencies in the vicinity of 100 Hz. The maximum value of dielectric constant ε observed for the BST0.2 thin film is 121 at a frequency about 100 Hz. However, from Fig. 5(a), it observed that the dielectric loss (tan δ) for BST0.2 also decreases with an increase in frequency up to 1 MHz. There is very low dispersion in tan δ in the higher frequency range. The values of dielectric loss are also seen to be very low.

From Fig. 5(b), it is observed that the dielectric constant ε decreases continuously with an increase in frequency for BST0.3 thin film, while the variation of tan δ with frequency shows a relaxation peak in the vicinity of 1.2 kHz. It is seen that there is no prominent variation in tan δ in the frequency range of 1.5–15 KHz, however, tan δ again increases with frequency above 15 KHz. The transition temperature of BST0.3 is in the below room temperature hence the variation of tan δ with a frequency show anomalous behavior. It is observed that the overall values of tan δ are less than 0.06 in all observed frequency range for BST0.3 thin film; it is observed that the frequency dispersion is very low and this is a prime requirement of good ferroelectric materials. Dielectric properties (ε) of BST films may vary in composition, thickness, precursors, and heat treatment temperatures.[19–22] From the dielectric constant, it is seen that the good quality of thin-film shows low dispersion.[23,24]

Figures 6(a) and 6(b) show the variation of dielectric constant (ε) and tan δ as a function of temperature for various frequencies for the BST0.2 thin film, respectively. From Fig. 6(a), it is seen that the variation of dielectric constant (ε) as a function of temperature shows a ferroelectric to paraelectric peak in the vicinity of 42 °C for lower frequencies, while for higher frequencies, there is no prominent variation in the dielectric constant ε with temperature. From Fig. 6(b), it is observed that there are relaxation peaks in the vicinity of 42 °C in the variation of tan δ with temperature for various frequencies. However, this effect is not prominent for higher

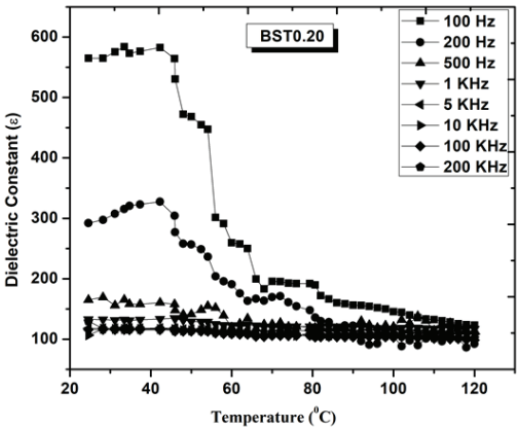

(a)

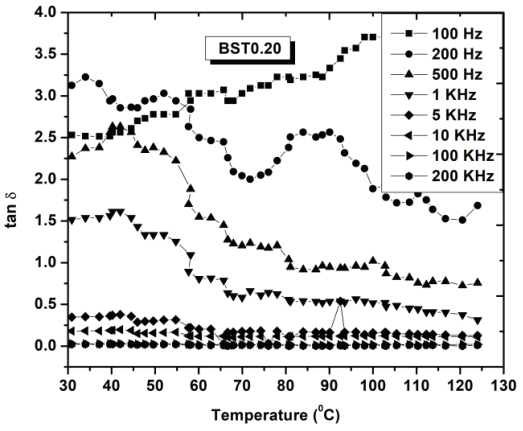

(b)

Fig. 6. (a) Variations dielectric constant (ε) with temperature for BST0.2. (b) Variations loss tangent (tan δ) with temperature for BST0.2.

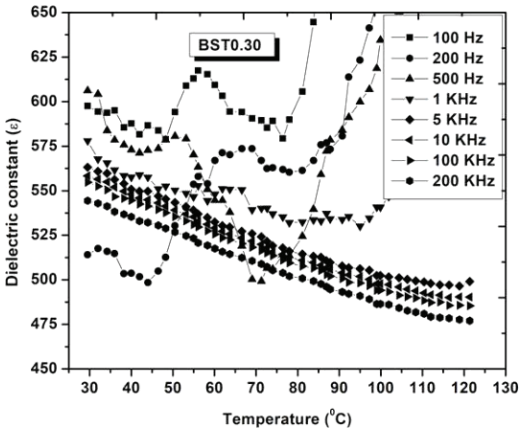

(a)

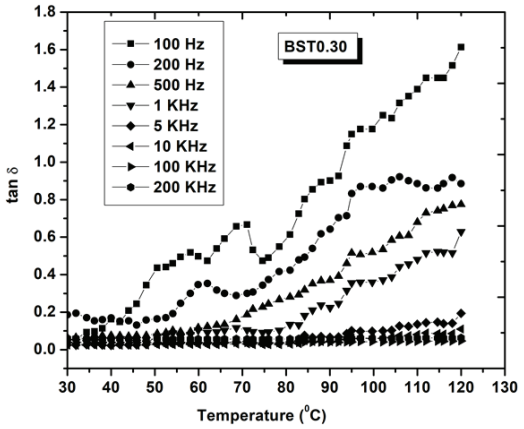

(b)

Fig. 7. (a) Variations dielectric constant (ε) with temperature for BST0.3. (b) Variations loss tangent (tan δ) with temperature for BST0.3.

frequencies. From Fig. 6(b), it is also observed that there are ups and downs in the variation of tan δ for a small interval of temperature at lower frequencies. It may be attributed due to electrode effect, crystal imperfection, or space charge polarization.[23,25,26]

Figures 7(a) and 7(b) show the variation of dielectric constant (ε) and tan δ as a function of temperature for various frequencies for the BST0.3 thin-film, respectively. From Fig. 7(a), it is observed that initially dielectric constant ε decreases with temperature for BST0.3 thin film.[23] For temperature greater than 40 °C, the variation of dielectric constant ε with temperature shows anomalous behavior for BST0.3 Thin film at lower frequencies. From Fig. 7(a), it is seen that the dielectric constant ε increases with temperature. However, it is seen that the dielectric constant continuously decreases with temperature for frequency ≥1 kHz. Hence, this type of relaxation in the vicinity of room temperature, in the variation of dielectric constant ε with temperature indicates that the transition temperature for BST0.3 may occur just below room temperature. This result matches well with earlier reports.[20–23] Sutar *et al*. reported that bulk BST.2 and BST0.3 ceramics showed a peak located at 58 °C and 30 °C, respectively.[23] It is known that a ferroelectric property depends on microstructure, especially with respect to grain size.[16,22] From Fig. 7(b), it is seen that tan δ increases with temperature for frequencies 100 Hz, 200 Hz, 500 Hz, and 1 kHz, while it remains constant for frequencies greater than 1 kHz. Here it is observed that the increases in dielectric constant (ε) with temperature (T) occur for frequencies below 1 kHz only and $d\varepsilon/dT$ decreases with an increase in frequency. These features occur due to the existence of interfacial polarization at grain–grain boundary interface. Bidaut *et al*. and Choi *et al*. reported that the grain–grain boundary interface occurs probably due to fractional Ti^{3+} acceptor state in the bulk of grain. It is similar to earlier report.[23] The experimental behavior is a good occurrence between the dielectric relaxation and the electrical conduction of the relaxing species.[23]

7. Impedance Spectra

The dielectric properties of ferroelectric materials are affected by various factors like charge displacement, dipole reorientation, space charge formation, interfacial polarization

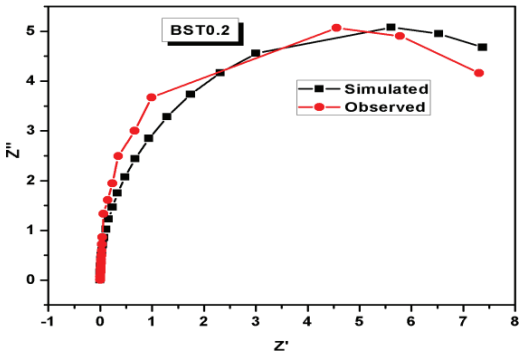

(a)

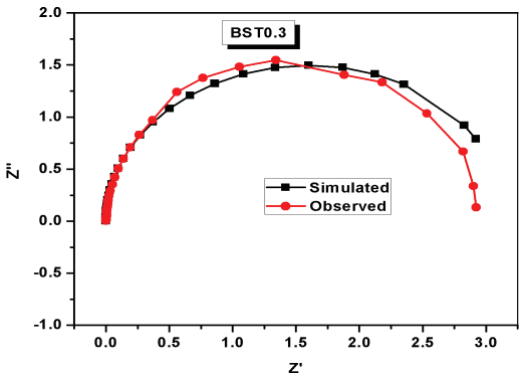

(b)

Fig. 8. Variation of Z'' as a function of Z' for (a) BST0.2 and (b) BST0.3 thin films.

Table 1. Variation of R, ω, and interfacial capacitance in model circuit for BST0.2 and BST0.3.

Composition	ω_{01}	ω_{02}	R_1 (MΩ)	R_2 (MΩ)	C_i (pf)
BST0.2	1300	2800	9	1.5	200
BST0.3	3500	7500	2.35	0.8	0

between two layers or two grains, DC conductivity term σdc, Debye relaxation, electrode effect, etc. The method of complex impedance analysis has emerged as a very powerful tool for separating out these contributions. The complex impedance Z^* is given by the following equation :

$$Z^* = Z' - jZ'',$$

where Z', Z'' are the real and imaginary parts of Z^*.

Figures 8(a) and 8(b) show the observed and simulated impedance spectra for BST0.2 and BST0.3 thin films. Figures 8(a) and 8(b) show the best possible curve fitting for the BST0.2 and BST0.3 thin films. The modified Maxwell–Wagner model is used for impedance curve fitting. It consists of two R-C circuits and interfacial capacitance C_i in series. The impedance fitting parameters are given in Table 1.

8. Conclusion

Barium Strontium Titanate $(Ba_{1-x}Sr_x)TiO_3$ ($x = 0.2$ and 0.3) was successfully deposited on $Pt/TiO_2/SiO_2/n$-si (100) substrates by the method of dip and dry technique. The X-ray spectra show BST thin films are pseudo cubic crystal structure with a tetragonal distortion. The Raman spectroscopy was used to examine the structure of BST thin film. Dense, homogenous and crack-free BST thin films with uniform thickness and uniform grain size were produced at 730 °C for 1 h. The electrical characteristics of the thin films showed a good dielectric constant with low dispersion. The phase transition from tetragonal-to-cubic in the $Ba_{0.7}Sr_{0.3}TiO_3$ thin film is about just below room temperature with a maximum dielectric constant of 578 at 1 kHz. Impedance spectroscopy study gives valuable information about the grain boundary interactions in the BST0.2 and BST0.3 thin film layers.

Acknowledgments

All Authors are thankful to the DRDO-NRB, New Delhi authority for Financial Support to the research work. Also, the authors sincerely thank Dr. V. L. Mathe, Associate Professor, Department of Physics, Savitribai Phule Pune University, Pune, for providing Raman facility.

References

[1]P. Li, T.-M. Lu and H. Bakhru, High charge storage in amorphous $BaTiO_3$ thin films, *Appl. Phys. Lett*. **58**, 2639 (1991).

[2]L. M. Sheppard, Advances in processing of ferroelectric thin films, *Am. Ceram. Soc. Bull*. **71**, 85 (1992).

[3]L. Huang, Z. Chen, J. D. Wilson S. Banerjee, R. D. Robinson, I. P. Herman, R. Laibowitz and S. O'Brien, Barium titanate nanocrystals and nanocrystal thin films: Synthesis, ferroelectricity, and dielectric properties, *J. Appl. Phys*. **100**, 034316 (2006).

[4]M. Jain, S. B. Mujumdar, R. S. Katiyar and A. S. Bhalla, Novel barium strontium titanate $Ba_{0.5}Sr_{0.5}TiO_3$/MgO thin film composites for tunable microwave devices, *Mater. Lett*. **57**, 4232 (2003).

[5]J. Zhai, X. Yao and H. Chen, Structural and dielectric properties of $Ba_{0.85}Sr_{0.15}(Zr_{0.18}Ti_{0.85})O_3$ thin films grown by a sol–gel process, *Ceram. Int*. **30**, 1237 (2004).

[6]L. N. Gao, J. W. Zhai, X. Yao and Z. K. Xu, Dielectric properties of heterostructured BZT thin films prepared by sol–gel technique, *Mater. Lett*. **62**, 3198 (2008).

[7]A. N. Tarale, S. R. Jigajeni D. J. Salunkhe P. B. Joshi, S. B. Kulkarni, D. M. Phase, R. J. Chaudhary and S. K. Deshapande, Synthesis and characterization of $Ba_{0.7}Sr_{0.3}TiO_3$, $BaZr_{0.3}Ti_{0.7}O_3$ thin film heterostructures, *J. Mater. Sci. Mater. Electron*. **23**, 557–566 (2012).

[8]Q. X. Jia, H. H. Kung and X. D. Wu, Microstructure properties of $Ba_{0.5}Sr_{0.5}TiO_3$ thin films on Si with conductive $SrRuO_3$ bottom electrodes, *Thin Solids Films*, **299**, 115 (1997).

[9]M. Nayak, S. Y. Lee and T.-Y. Tseng, Electrical and dielectric properties of $(Ba_{0.5}Sr_{0.5})TiO_3$ thin films prepared by a hydroxide–alkoxide precursor-based sol–gel method, *J. Mater. Chem. Phys*., **77**, 34–42 (2002).

[10]A. Piorra, A. Petraru, H. Kohlsted M. Wuttig and E. Quand, Piezoelectric properties of $0.5(Ba_{0.7}Ca_{0.3}TiO_3) - 0.5[Ba(Zr_{0.2}Ti_{0.8})O_3]$ ferroelectric lead-free laser deposited thin films, *J. Appl. Phys*. **109**, 104101 (2011).

[11]F. Techeliebou and S. Baik, Influence of the laser wavelength on the microstructure of laser ablated $Ba_{0.5}Sr_{0.5}TiO_3$ films, *J. Appl. Phys*. **80**, 7046 (1996).

[12]Y. C. Choi, J. Lee and B. S. Lee, Improvements of the properties of chemical-vapor-deposited (Ba, Sr) TiO_3 films through use of a seed layer, *Jpn. J. Appl. Phys*. **36**, 6824 (1997).

[13]S. Kim and S. Baik, Effects of surface structures of MgO(100) single crystal substrates on ferroelectric $PbTiO_3$ thin films grown by radio frequency sputtering, *J. Vac. Sci. Technol. A*. **13**, 95 (1995).

[14]B. Fu, Y. Yang, K. Gao and Y. Wang, Significant increase of Curie temperature and large piezoelectric coefficient in $Ba(Ti_{0.80}Zr_{0.20})$-O_3-$0.5(Ba_{0.70}Ca_{0.30})TiO_3$ nanofibers, *Appl. Phys. Lett*. **107**, 042903 (2015).

[15]Y. Chen, T. Y. Zhang, Q. G. Chi, J. Q. Lin, X. Wang and Q. Q. Lei, Low temperature growth of (100)-oriented $Ba(Zr_{0.2}Ti_{0.8})O_3$-$0.5(Ba_{0.7}Ca_{0.3})TiO_3$ thin films using a $LaNiO_3$ seed layer, *J. Alloys Compd*. **663**, 818 (2016).

[16]F. M. Pontes, E. R. Leite, D. S. L. Pontes, E. Longo, E. M. S. Santos, S. Mergulhao, P. S. Pizani, F. Lanciotti Jr., T. M. Boschi and J. A. Varela, Ferroelectric and optical properties of $Ba_{0.8}Sr_{0.2}TiO_3$ thin film, *J. Appl. Phys*. **91**, 5972 (2002).

[17]G. Burns, J. A. Sanjurjo and E. Lopez- Cruz, High-pressure Raman study of two ferroelectric crystals closely related to $PbTiO_3$, *Phys. Rev. B* **30**, 7170 (1984).

[18]J. D. Freire and R. S. Katiyar, Lattice dynamics of crystals with tetragonal $BaTiO_3$ structure, *Phys. Rev. B* **37**, 2074 (1988).

[19]N. V. Giridharan, R. Jayavel and P. Ramasamy, Structural, morphological and electrical studies on barium strontium titanate thin films prepared by sol–gel technique, *Crystal Res. Technol.* **36**(1), 65 (2001).

[20]J. G. Cheng, X. J. Meng, B. Li, J. Tang, S. L. Guo, J. H. Chu, M. Wang, H. Wang and Z. Wang, Ferroelectricity in sol-gel derived $Ba_{0.8}Sr_{0.2}TiO_3$ thin films using a highly diluted precursor solution, *Appl. Phys. Lett*. **75**, 2132 (1999).

[21]C. B. Parker, J.-P. Maria and A. I. Kingon, Temperature and thickness dependent permittivity of (Ba,Sr)TiO_3 thin films, *Appl. Phys. Lett*. **81**, 2 (2002).
[22]D. O'Neill, G. Catalan, F. Porras, R. M. Bowman and J. M. Gregg, Thin film ferroelectrics for capacitor applications, *J. Mater. Sci. Mater. Electron*. **9**, 199 (1998).
[23]M. M. Sutar, A. N. Tarale, S. R. Jigajeni, S. B. Kulkarni and P. B. Joshi, Investigations on nanocrystalline BST-LSMO magnetodielectric composites, *Appl. Nanosci*. **2**, 311 (2012).
[24]S. G. Chavan, A. N. Tarale, P. M. Kharade, S. B. Kulkarni and D. J. Salunkhe, Micro-wave sintered nickel doped cobalt ferrite nanoparticles prepared by hydrothermal method, *J. Chin. Adv. Mater. Soc*. **5**, 47 (2017) .
[25]O. Bidaut, P. Goux, M. K. Chikech, M. Belkaoumi and M. Manglion, Space charge relaxation in perovskite, *J. Phys. Rev. B*. **49**, 7868 (1994).
[26]S. K. Choi, B. S. Kang, Y. W. Cho and Y. M. Vysochanskii, Diffuse dielectric anomaly in ferroelectric materials, *J. Electroceram*. **13**, 493 (2004).